Comments on Inorganic Chemistry
Publication details, including instructions for authors and subscription information:
http://www.informaworld.com/smpp/title~content=t713455155

X-RAY POWDER DIFFRACTION CHARACTERIZATION OF POLYMERIC METAL DIAZOLATES

Norberto Masciocchi[a]; Simona Galli[a]; Angelo Sironi[b]
[a] Dipartimento di Scienze Chimiche e Ambientali, Università dell'Insubria, Como, Italy [b] Dipartimento di Chimica Strutturale e Stereochimica Inorganica, Università di Milano, Milano, Italy

To cite this Article Masciocchi, Norberto , Galli, Simona and Sironi, Angelo(2005) 'X-RAY POWDER DIFFRACTION CHARACTERIZATION OF POLYMERIC METAL DIAZOLATES', Comments on Inorganic Chemistry, 26: 1, 1 — 37
To link to this Article: DOI: 10.1080/02603590590920361
URL: http://dx.doi.org/10.1080/02603590590920361

Comments on Inorganic Chemistry, 26: 1–37, 2005

ISSN: 0260-3594 print
DOI: 10.1080/02603590590920361

Taylor & Francis
Taylor & Francis Group

X-RAY POWDER DIFFRACTION CHARACTERIZATION OF POLYMERIC METAL DIAZOLATES

NORBERTO MASCIOCCHI
SIMONA GALLI

Dipartimento di Scienze Chimiche e Ambientali, Università dell'Insubria, Como, Italy

ANGELO SIRONI

Dipartimento di Chimica Strutturale e Stereochimica Inorganica, Università di Milano, Milano, Italy, and Istituto di Scienze e Tecnologie Molecolari del CNR, Milano, Italy

Polymeric metal diazolates typically appear as insoluble and intractable powders, the structure of which could only be retrieved by the extensive use of *ab-initio* X-ray powder diffraction (XRPD) methods from *conventional* laboratory data. A number of selected examples from the metal pyrazolate, imidazolate, pyrimidin-2-olate and pyrimidin-4-olate classes are presented, highlighting the specific crystallochemical properties, material functionality and methodological aspects of the structure determination process. Linear and helical one-dimensional polymers, layered systems and three-dimensional networks are described, with particular emphasis on polymorphism and on the thermal, optical, magnetic and sorption properties. A brief outline of the method, as it has been tailored in our laboratories during the last decade, is also offered.

***Keywords*: powder diffraction, coordination polymers, metal diazolates, polymorphism, crystal structure**

Address correspondence to Norberto Masciocchi, Dipartimento di Scienze Chimiche e Ambientali, Università dell'Insubria, via Valleggio 11, 22100 Como, Italy. E-mail: norberto.masciocchi@uninsubria.it

INTRODUCTION

The knowledge of the "molecular" structure, in whatever aggregation state, is at the basis of the comprehension of physico-chemical properties, such as stability, inertness, magnetism, optics, etc., and can therefore be successfully employed to tune the mentioned properties when tailored systems are sought. The amount of structural information gathered in the last decade by conventional X-ray single-crystal techniques has allowed the estimation of important stereochemical features (geometrical parameters) as well as the interpretation of energetic barriers, the assessment of the correct chiralities, the development of bonding theory and, above all, the discovery of new classes of compounds, which chemical analysis or spectroscopy alone could not have revealed. Thus, single crystals (studied either by X-ray or neutron diffraction) are, and will continue to be, the primary source of this information.

However, many materials only appear as polycrystalline species and their structural characterization must rely on powder diffraction data, with the obvious difficulties inherent in the partial and complex sampling of the scattered intensity of a 3D reciprocal lattice squeezed onto a 1D space.[1] Only in the last decade, instrumentation and software for X-ray Powder Diffraction (XRPD) analysis reached a level of quality permitting the *ab-initio* structural analysis of several hitherto unknown structures of inorganic, organic and organometallic species, all together adding to less than a mere 0.3% of the deposited structures (CSD and ICSD). While refinement of predetermined models (of a few independent atoms) was already within the structural chemist's hands after the Rietveld and the so called "two-stage" methods were proposed, for X-rays, in the 1980s, it was not until recently that more complex structures could be studied by XRPD, opening the way to the crystallographic analysis of several new classes of compounds.

Our group has been interested, in the last 15 years, in the chemistry and structural characterization of several metal complexes containing polydentate aromatic nitrogen ligands, for their specific reactivity towards simple heterocumulenes, and, later, organic moieties catalytically transformed by these (typically polynuclear) systems. During these studies, we learned of the existence of yet uncharacterized intractable species, which opened the way to an extensive project in which several polymeric compounds, of different nature, topology and physical

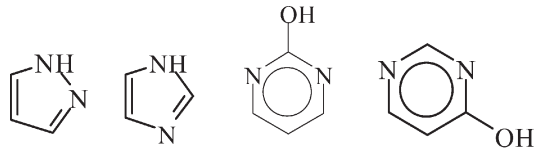

Hpz Him 2-pymoH 4-pymoH

Scheme 1.

properties were prepared and fully characterized. Their brief structural description, reported in the following paragraphs, will be coupled to the most significant findings, which span from surprisingly high thermal inertness, to polymorphism, intercalation, sorption, magnetic and (non linear) optical properties.

Worthy of note, all these systems have been characterized by XRPD on conventional laboratory data, showing the viability of the method for the determination of (otherwise inaccessible) structural features, and, in several cases, even of the correct stoichiometry. The amount of work reported in the following pages spans the whole last decade and nicely shows that a **complete** class of homologous (insoluble, but polycrystalline) species (in this case, metal diazolates) could be successfully studied by XRPD, opening the way to new and important chemistry, initially unforeseen, until the stereochemical rules and proper engineering of the materials were devised.

With reference to Scheme I, where a schematic drawing of the heterocyclic ligands, in their neutral forms, is depicted, shortened names will be used throughout the paper, such as pz for pyrazolate, im for imidazolate and X-pymo for pyrimidin-X-olate $(X = 2, 4)$.

Brief Description of the *ab-initio* XRPD Technique, as Implemented and Developed in our Laboratories (1991–2004)

In the last decade, we have been active in adapting, and extensively using, experimental and computational methods which allowed, *from conventional powder diffraction data only*, to retrieve that minimal amount of structural information which, coupled with other ancillary data, can satisfactorily answer questions such as: What is the stoichiometry of the sample? What is its crystal and/or molecular structure (in terms of connectivity pattern)? What are the supramolecular features and the

structural relations among the different asymmetric units and/or molecular fragments?

Obviously, these (and other) questions can be much more accurately addressed by conventional single-crystal diffraction analysis, which is faster, cheaper, easier to perform and nowadays included in several practical classes at different university levels and careers. Thus, if a single-crystal of the species under study is available, it should be (at least initially) used as such in diffraction experiments. In the unfortunate cases where monocrystals cannot be grown, then XRPD is the method of choice, provided that the structural complexity (addressed by the number of non-hydrogen atoms in the asymmetric unit, N_{at}) is not too high ($N_{at} < 40$). As of August 2004, *i.e.* about 10 years after the introduction, and diffusion, of the method, the number of crystal structures of molecular compounds (organic and organometallic species) determined by this method barely reaches a few hundreds, *i.e.* a mere 0.1% of the entries of the Cambridge Structural Database. However, the growing interest in this technique is witnessed by the appearance, in the recent literature, of several review papers, focusing on the different methodological aspects of *ab-initio* XRPD, as well as of a few dedicated monographs or books; for the sake of simplicity, the reader is redirected to the most recent books on the subject[2] and to a collection of minireviews on XRPD studies of molecular functional materials.[3]

Without going into the details of the overall structure analysis process, the following points should complement the information inserted in the original structural papers cited below and trace a line of "good practice," which, differently from single-crystal analyses, is often abandoned, or twisted, depending on the specific problems encountered in specimen preparation, size, stability and (para)crystallinity:

- About 30 mg (or more) of a monophasic polycrystalline species should be gently crushed, and eventually sieved, down to the 1–10 μm range; sample holders with minimal background contribution (zero background plates) should be employed and filled, up to the reference rim, by the powder, either in dusting or side loading mode. The use of inert binders is sometime helpful.
- Well aligned conventional diffractometers with monochromatized radiation (typically, Cu-Kα) and narrow optics must be used for data collection (typically, in step scan mode, $\Delta 2\theta = 0.02^\circ$, $5 < 2\theta < 100^\circ$;

$t = 10-30\,\mathrm{s\ step^{-1}}$). If the sample is transparent to X-rays, very accurate peak positions for indexing can be obtained by a second tailored data collection on a very thin film.

- Peak search and/or profile fitting should normally afford accurate positions ($\Delta 2\theta < 0.02^\circ$) of at least 20 peaks, later fed to automatic indexing programs. Usually, a combination of different strategies should be used to increase the confidence on the (often multiple and unclear) results. Whole pattern structureless profile matching (Le Bail or Pawley's methods) must be used for cell confirmation, space group determination and (integrated) intensity extraction.
- Structure solution can be performed by conventional (Patterson or Direct) reciprocal space methods, although real space techniques (scavengers, Monte Carlo, simulated annealing and genetic algorithms) are now prevailing.
- Completion and refinement of the final structural, microstructural and *instrumental* models are normally performed by whole profile matching (Rietveld method). Inclusion of geometrical restraints (bond distances, angles, torsions, planarity, etc.) can be required in order to stabilize convergence to physically sound values.
- More then ever, careful reconsideration of the results obtained at each step should be done, making the whole process not straightforward but, rather, iterative. Not infrequently, new sample preparations, purification, deposition, etc., are required in order to "correct" non-ideality of the original sample and to include a minimal set of correction terms.
- The different profile and integrated intensity agreement factors, which, differently from conventional single-crystal analyses, are not straightforwardly interpreted, should be estimated. Visual analysis of the matched profile and of the structure derived there from, with particular emphasis on *inter*molecular contacts as an estimate of the structure correctness, must be carried on.

Much like a culinary recipe, which must not be strictly followed in order to prepare excellent gourmet dishes, the art of structural analysis also greatly benefits from a balanced mixture of experience, intuition, curiosity, perseverance (*if not stubbornness*) and diversity of the tools and of the methods employed. This is particularly true when constantly occurring new instrumental artifacts afford less-than-optimal data, and preferred orientation, absorption and optical aberration effects, or

sample instability, thermal drifts, beam misalignment and other somewhat unpredictable, but subtle, source of errors, are present.

A. Metal Pyrazolates

The first class of compounds that will be discussed hereafter is based on the pyrazolate anion (pz), the chemistry of which has been thoroughly investigated in the last 30 years, with particular emphasis on its ability to act as a prototypical N,N′-*exo*bidentate ligand, thus favoring the construction of polynuclear metal complexes (with the metals kept at distances typically below 3.5 Å);[4] although more exotic coordination modes (monodentate, η^2, η^5 and even more complex ones) have been recently observed for substituted pz species (particularly when bulky substituents are present in the 3,5-positions[5] or when lanthanides are employed[6]), the following examples, in which the simple, *unsubstituted*, pyrazole is used as starting material, all *invariably* show bridging pz anions. These species were among the first we characterized by *ab-initio* XRPD methods, and, beyond being benchmark cases for the development of this structural technique, allowed the discovery of subtle structural effects such as polymorphism and stability patterns, later confirmed during our studies on the imidazolate and pyrimidinolate polymers discussed below.

Interestingly, among the heterocyclic anions presented here, pz is the only one that can possibly lead to multiple bridges, since virtually no atom is present between the metal ions (bridged by a N,N′-*exo*bidentate pz ligand), thus opening the possibility of forming one-dimensional chains, even if metals in +II or +III oxidation states are employed. Worthy of note, a rhodium dimer bridged by *four* pyrazolates is known,[7] but this *unique* occurrence was not found among our samples.

A_1. Buchner's "Silber Salz"[8]. The Cu(pz) and Ag(pz) species have been long known[9] but, until 1994, their oligomeric or polymeric nature had never been clearly demonstrated. In our seminal paper,[10] we were able to recognize four different phases, namely: α- and β-Cu(pz), and α- and β-Ag(pz), the structures of which are drawn in Figures 1 and 2; our XRPD analysis clearly showed that α-Cu(pz), and α-Ag(pz) are isomorphous species, containing polymeric 1D chains based upon linearly coordinated M(I) ions and brigding pz ligands, zigzagging through the crystal in an *all-trans* conformation; β-Cu(pz) itself was also found to

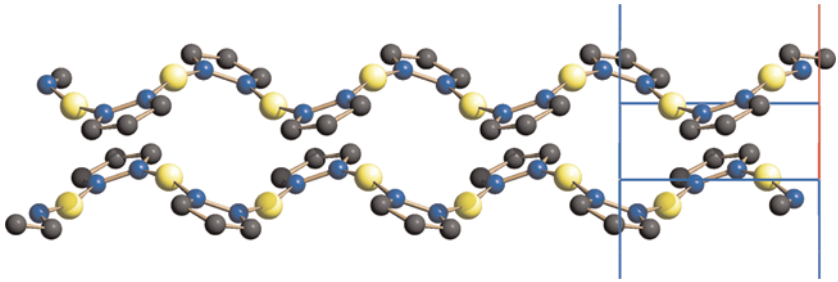

Figure 1. Schematic drawing of the M(pz) polymeric chains present in α-Cu(pz), and α-Ag(pz). In β-Cu(pz), the chains come slightly closer, in pairs, but possess nearly identical conformation.

be based on the same structural motif, although crystallizing in a different packing environment. However, the determination of the molecular structure of β-Ag(pz) (which was later formulated as $[Ag(pz)]_3$) proved to be more difficult, since, while we were working on this problem, we believed for a long time that β-Cu(pz) and β-Ag(pz) were also a couple of isomorphous compounds: indeed, the XRPD pattern of β-Ag(pz) and that of β-Cu(pz) show some similarities, particularly when a few unindexed peaks in the former are attributed to an impurity. Thus, we repeatedly attempted to refine the structural model obtained for β-Cu(pz) using the spectrum of β-Ag(pz). Being unable to obtain a

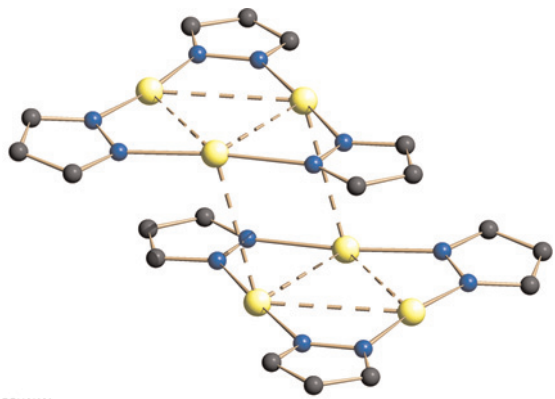

Figure 2. Schematic drawing of the $[Ag(pz)]_3$ trimers. Short *intra*- and *inter*molecular contacts are evidenced as fragmented lines. (The color image is available online at www.taylorandfrancis.com).

reasonable agreement and after many failed attempts to obtain a "pure" $[Ag(pz)]_n$, phase, we decided to reconsider the problem by allowing for a larger cell in the indexing procedure. We soon realized that there was a cell, with a volume *ca.* 3/2 larger than that of β-Cu(pz), accounting for all the observed peaks of the spectrum.[11] [Obviously, other diffraction techniques (*e.g.*, selected-area electron diffraction) could help in assigning the correct lattice metrics if a (suitably oriented) microcrystal is found.] Direct methods[12] eventually lead to the correct formulation of β-Ag(pz) as a cyclic, trimeric compound that was readily modelled in the structure completion and refinement stages by imposing the proper geometrical restraints.

The polymorphic nature of samples α- and β-Cu(pz), as shown in Figure 3, is related to the pairing of adjacent copper pyrazolate chains in β-Cu(pz), and to the formation of a pseudohexagonal packing of these "pairs," markedly different from the rectangular motif observed in the α-phase.

The structural analysis briefly presented above already contains a few important methodological aspects, inherent in the XRPD method, i.e.: i) the strict[13] requirement on the availability of a crystallochemically pure species (or the belief in the monophasic nature of the sample)[14]; ii) the misconceptions raised by wrong perspectives or hypotheses and, finally, iii) the necessity of restraining the bonding parameters of stiff fragments of known geometry to chemically sound values (given the absence of significant accurately measured intensities at medium and high-2θ values). From this example it is clear that XRPD alone allowed a strong chemical and structural belief [the isomorphism of β-Cu(pz) and β-Ag(pz)] to be discarded and led to the proposal of a totally different structural model for $[Ag(pz)]_3$.

A_2. Magnetically Active One-dimensional Polymers. Polymeric materials possessing spin-crossover (SC) or spin-transition (ST) behaviors at, or near, room temperature, which are particularly appealing in the development of nanodevices, sensors, etc., have been recently synthesized and spectroscopically, thermally and magnetically characterized; within this class of compounds, Fe(II)-complexes, bridged by polyazaheterocycles, appeared as versatile and promising species.[15,16] Their interesting functional properties have been attributed to the cooperativity of subtle effects, such as the *collinear* geometry of the active centers and the rigidity of the whole one-dimensional framework, greatly

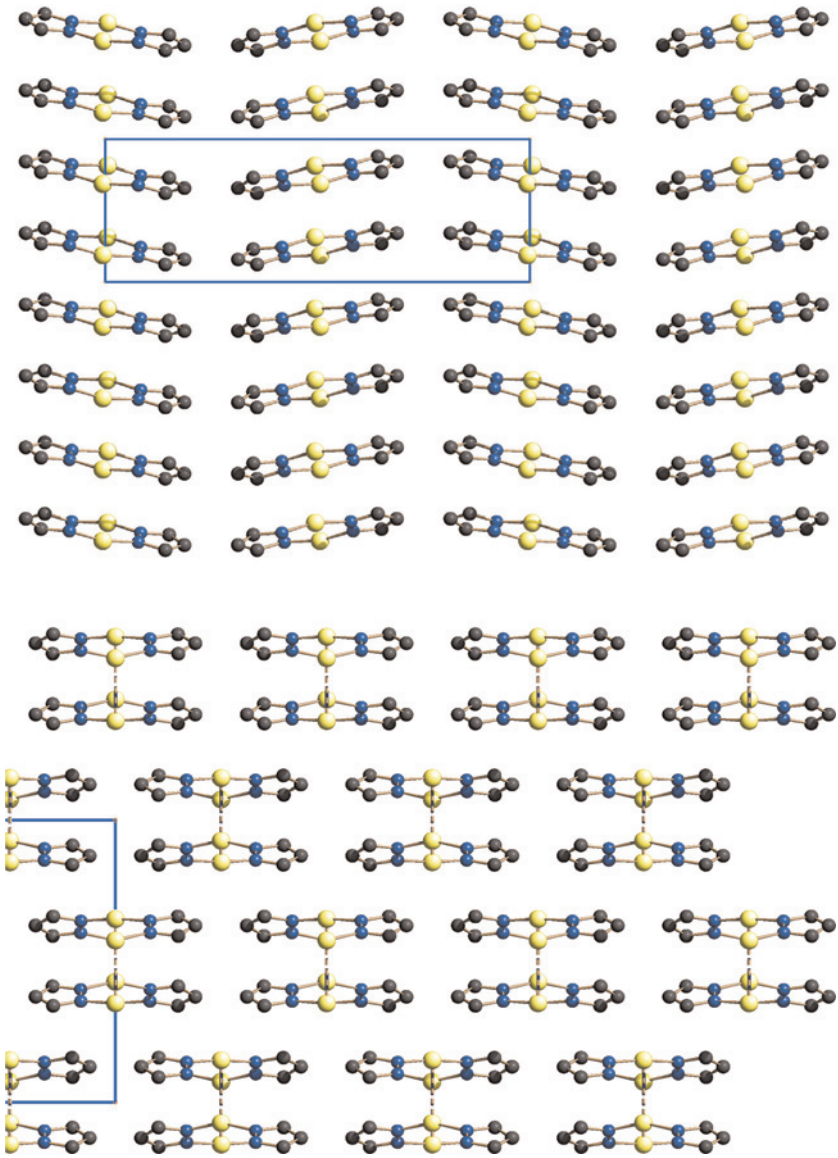

Figure 3. Schematic drawing of the crystal packing of the Cu(pz) polymeric chains in the α- (top) and β-phases (bottom). The 1D chains run perpendicularly to the plane of the drawings, thus misleadingly appearing as dimeric entities. Short contacts (vertical fragmented lines) are evidenced in β-Cu(pz). (The color image is available online at www.taylorandfrancis.com).

enhancing (by electron-phonon coupling) their magnetic response, spin-transition features[17] and even photomechanical effects.[18] However, their chemical and thermal stability is limited by the presence of counterions, balancing, in the solid state, the net positive charges of the $[(FeL_3)^{2+}]_n$ chains (typically, L = 4-substituted triazoles). Moreover, since these species generally afford materials with low crystallinity[19] and tend to behave very differently as the result of even small differences in preparation, their structural characterization could not adequately be performed. Thus, only indirect evidences, such as IR, Raman, Mössbauer and EXAFS spectroscopy or structure models of the corresponding oligomeric species[20] or of vaguely related polymers,[21] are available.[22]

Aiming to the comprehension of the structural features of these complex polymers, we prepared the $Fe(pz)_3$, $Co(pz)_3$, $Co(pz)_2$ and $Ni(pz)_2$ *model* systems. Their XRPD characterization showed that binary metal pyrazolates tend to afford highly crystalline species where *strictly collinear* chains of metal atoms are present (see Figure 4);[23,24] in addition, $Ni(pz)_2$ was found to be polymorphic, since two phases [α (orthorhombic) and β (monoclinic), depending on the synthetic strategy adopted] were detected. Some of the basic topologies of these chains are not new and can be related to the archetypic β-$RuBr_3$ (or anhydrous scandium acetate) and $BeCl_2$ phases [Fe(III)/Co(III) and Fe(II)/Co(II)/Cu(II)/Zn(II), respectively]; on the contrary, we are not aware of simple binary species adopting, in the solid state, the wavy chain structure of both $Ni(pz)_2$ phases.

The structures of these species, although *not* unexpected, are, however, the *direct* proof of the multiple linkages sustained by the polypyrazolate bridges in all analogous, related polymeric chains; moreover, since *all* metal atoms lie (in a variety of space groups!) on special positions, the final refinements also allowed the assessment of several stereochemical features with high accuracy. The anisotropic disposition of the metals in the crystal lattice suggests that the strongest electronic and, eventually, magnetic coupling in these systems are imputable to the poly-pyrazolate-bridged M···M contacts, and not to interchain interactions, which might be at work only at very low temperatures.[25] Thus, such direct linkages of the metal centers and their collinear geometrical arrangement are likely to cause the large cooperativity of the magnetic interactions, as witnessed by the considerable hystereses found in a number of structurally related, but more complex, polymeric materials.[26,27]

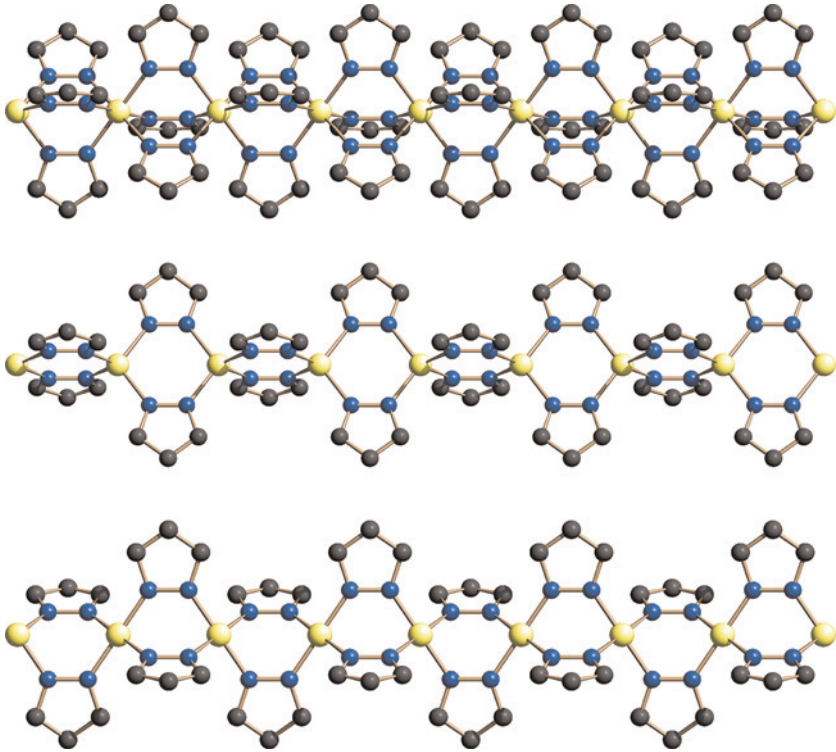

Figure 4. Schematic drawing of the $M(pz)_n$ polymeric chains. Top to bottom: $Fe(pz)_3$, $Co(pz)_2$ and $Ni(pz)_2$. In the two polymorphs of the latter, identical chains pack in pseudohexagonal (α) or pseudorectangular (β) fashion. In *all* cases, metal atoms are strictly collinear. (The color image is available online at www.taylorandfrancis.com).

Worthy of note, lipophilic cobalt(II) triazole complexes bearing long alkyl chains in 4-positions, structurally related to the homoleptic $Co(pz)_3$ polymer, have been very recently prepared, and showed interesting gelification and thermochromic structural transitions;[28] since these features have been attributed to the presence of different equilibria, involving oligomeric and polymeric species, XRPD on (suitably simplified) species could provide a structural basis for the observed behavior.

Obviously, the complexity of the materials that can be studied by XRPD methods must not be too high. If the species under investigation does not easily afford crystals for conventional analysis, nor monophasic powders of polycrystalline nature, then the preparation of model systems, simplified in order to allow a successful structural characterization,

is a mandatory step, provided that the idealization is not too extreme nor does it change the sought structural features.[29] Indeed, this approach has already been used by us in the effort of understanding the reaction mechanism of CO_2 insertion in a complex organometallic species, substituting one phenyl group by a smaller $-CH_3$ residue, and fully characterizing the reaction intermediate by XRPD.[30]

A_3. Polycationic Polymeric Species. Most of the homoleptic metal pyrazolates described above (and in the related literature) have been synthesized from commercially available metal salts (chlorides, sulfates, nitrates, acetates, etc.) and the heterocyclic ligand (in its neutral form) dissolved in water, upon addition of bases (typically, ammonia or organic amines); before precipitation of the $M(pz)_n$ systems, *i.e.* before raising the pH value above 7, metal complexes of uncertain formulation are likely present in solution, and only the removal of the slightly acidic proton of pyrazole allows the quantitative recovery of the cited polymers. Worthy of note, the preparation of group 11 metal pyrazolates follows a different route, since *i*) Ag(I) *alone* induces the deprotonation of the coordinated ligand (pyrazole, imidazole, etc.) through the formation of suitable N-Ag bonds, and does not require the addition of an external base; ii) Cu(I), which is unstable in aqueous media, is used either as tetrakis-acetonitrile complex or prepared *in situ* from solid Cu_2O in molten pyrazole.

Within this context, we surprisingly found that the reactions of Group 12 metals (in their +II oxidation state), easily leading to the target polymers for zinc and cadmium,[24b] *quantitatively* form the $Hg(pz)NO_3$ phase if $Hg(NO_3)_2$ is employed. To our surprise, this was the first mixed-anion metal-pyrazolate ever prepared. Eventually, in a later study,[31] we demonstrated that imidazole reacts in the very same manner, leading to a species of $Hg(im)NO_3$ formulation. The reason for such behavior is easily explained if the crystal and "molecular" structures of both phases (drawn in Figs. 5 and 6) are described.

Both phases contain linearly coordinated Hg(II) ions, bridged by N,N′-diazolates in their normal exobidentate mode (with Hg-N values slightly above 2.0 Å), thus forming one-dimensional $[Hg(\mu\text{-}pz)]_n^{n+}$ or $[Hg(\mu\text{-}im)]_n^{n+}$ chains running throughout the crystals. The nitrate ions are hosted in the crystal lattice, between these polycationic chains; however, weak Hg $\cdots$ O contacts (above 2.75 Å) are present in the plane normal to the Hg-N vectors, possibly favoring the sudden precipitation of

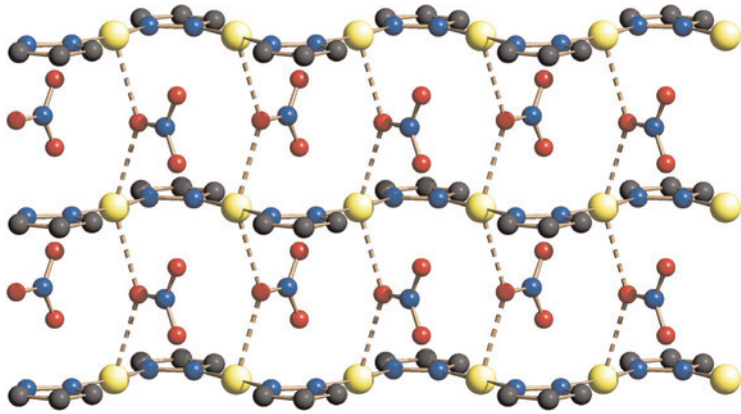

Figure 5. Schematic drawing of a portion of the $[Hg(pz)]_n^{n+}$ chain, surrounded by loosely interacting (dashed lines) nitrate ions.

these species during their synthesis, as if they were solids with an extensive three-dimensional nature. Although unexpected, this structural feature is also present in the fully inorganic mercury(II) hydroxo-nitrate, where the NO_3^- anions are completely embedded in a crystalline matrix generated by $[Hg(\mu\text{-}OH)]_n^{n+}$ polycations.[32]

Inter alia, the crystals of the $Hg(im)NO_3$ phase are non-centrosymmetric, P-62c: metal ions and imidazolates lie in special positions (two-fold axes), while two crystallographically independent NO_3^- anions (of

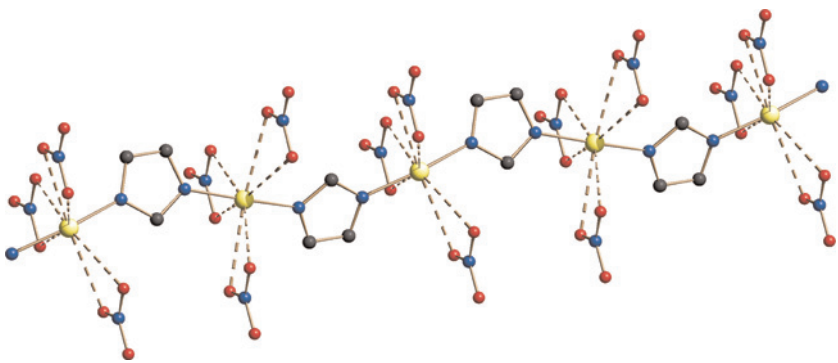

Figure 6. Schematic drawing of a portion of the $[Hg(im)]_n^{n+}$ chain, surrounded by loosely interacting (dashed lines) nitrate ions. (The color image is available online at www.taylorandfrancis.com).

different site symmetries) occupy the voids near the origin and on threefold axes at (2/3, 1/3, z). That this species is acentric was also confirmed by SHG measurements, its activity being 0.1 times that of urea (Kurtz-Perry powder technique).

Methodologically speaking, the structure determination of the $Hg(im)NO_3$ species, crystallizing in the hexagonal system, was not at all straightforward: indeed, in the high symmetry crystal systems, not only the Laue class is obscured by the exact coincidence of different classes of reflections, but even the trigonal-hexagonal dichotomy is not geometrically soluble and thus requires a multitude of parallel structure solution processes, possibly difficult to rank if heavy metal(s) (as in the present case) occupy pseudosymmetrical sites. Thus, more than ever, it's the overall structural consistence, rather than the ranking of the agreement factors, which helps during the whole process of model building. Obviously, at the end of the whole process, R factors reach, for the correct structural, microstructural and instrumental models, the lowest attainable values.

B. Metal Imidazolates

As an obvious extension of our studies on the metal pyrazolato systems, we later turned our attention to the coordination chemistry of the imidazolate anion (im), which has similar bonding ability but a bite angle favoring *exo*bidentate coordination of metals that lie about 5.6–6.0 Å apart. The variety of coordination modes found for imidazolate does not even approach the complexity recently found for the pyrazolate ligand since: *i*) the N,N′-*endo*bidentate mode (and its congeners) must be excluded on simple geometrical considerations, and *ii*) multiple bridges built on μ-im ligands are impossible. However, the limited coordination modes available to the imidazolate "anion" are overwhelmed by the torsional flexibility at the M-N bonds, thus allowing the existence of many different poly (2 or 3) dimensional frameworks if metal(II) ions are employed. Thus a single coordination (N,N′-*exo*bidentate) mode is likely to afford a wide(r) spectrum of "supramolecular" arrangements.

Our studies on the metal pyrazolate and imidazolate polymers are also propedeutic to the comprehension of other five-membered heterocyclic N-ligands: recently, the coordination chemistry of metal triazolato and tetrazolato (possessing 1,2- and 1,3-N,N′-connectivity, such as in pz and im, respectively) species have been reviewed,[33] and the possibility

of isolation of metal pentazolate systems (containing the elusive N_5^- cyclic anion) theoretically predicted.[34]

Moreover, imidazole and its derivatives are widely present in biologically active molecules, such as in the superoxide dismutase enzyme, where im bridges a Cu(II),Zn(II) pair;[35] thus the understanding of the stereochemical features of this ligand, coupled with its extensive spectroscopic and magnetic characterization, as well as of that of model systems, allows the study of its biological activity on a molecular basis.

B_1. Antimicrobially Active Polymers. Before our studies,[36] to our knowledge, the only reports of a species of the Ag(im) formulation appeared some decades ago,[37] while Cu(im) was never reported. Indeed, we attempted the syntheses of both silver and copper analogues, and successfully recovered a monophasic, air-stable Ag(im) species [but not Cu(im), which was a poorly diffracting, easily oxidizable white material].

Silver imidazolate was found to crystallize in acentric $P2_12_12_1$ (as also confirmed by powder SHG measurements[38]) and contains wavy one-dimensional chains hinged about short *inter*chain contacts (Ag· · ·Ag ca. 3.16 Å, see Figure 7). While in Ag(pz) the conformation of the 1D chain could be described by an *all-trans* pz-Ag-pz sequence, each Ag(im) polymer, still containing linearly coordinated silver ions, show a

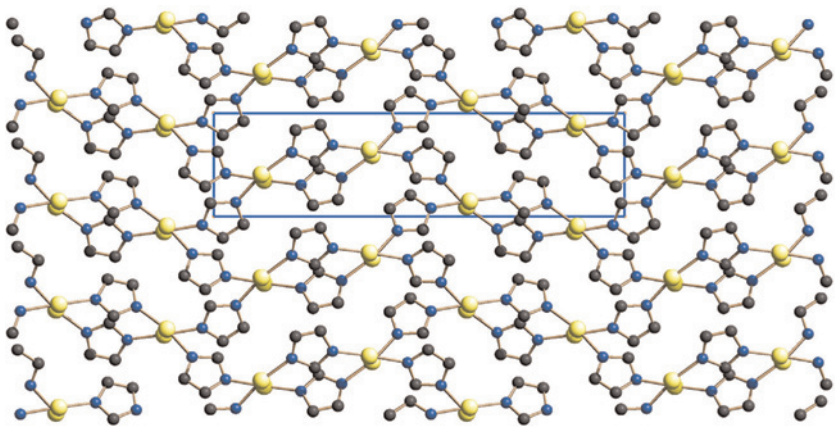

Figure 7. Schematic drawing of the crystal packing of Ag(im), viewed down [010]. The one-dimensional polymeric chains run nearly parallel to the horizontal cell axis, **c**. (The color image is available online at www.taylorandfrancis.com).

[*cis-trans*-] sequence interacting with several, not just two (below and above), adjacent chains. Differently from Ag(pz), the crystal packing of Ag(im) can be regarded as a herringbone arrangements of chains, stabilized by a complex network of d^{10}-d^{10} interactions.

After the publication of our paper, we learned of the interesting antimicrobial properties of the Ag(im) compound[39] and of some of its analogues (obtained by substituting the imidazolato group with other heterocyclic anions and/or introducing ancillary ligands): indeed, several Ag(I) salts are widely marketed as antifungal drugs and imidazole-based solutions are often employed in OTC pharmaceuticals. The occasional coupling of the two functionalities has therefore prompted the determination of its overall antibacterial activity which, among the many species of the same kind, resulted by large the most effective. For a detailed analysis and interpretation of these properties, refer to the work of Nomiya et al.[40]

Worthy of note, the poorly soluble Ag(im) species can be dissolved upon reaction with tertiary aromatic phosphines: subsequent solvent removal or crystallization generates the complex [$Ag(im)(PPh_3)$ and $Ag_2(im)_2(PPh_3)_3$] polymers;[41] differently, the Ag(pz) analogue was shown to afford, in the same conditions, dinuclear species only [$Ag_2(pz)_2(PPh_3)_2$ or $Ag_2(pz)_2(PPh_3)_3$].[42]

Ag(im) crystallizes in acentric $P2_12_12_1$, thus only a few peaks should be systematically missing (half of the axial reflection); however, in a rather unpredictable manner, the first clearly evident peak occurs at $2\theta \sim 17^\circ$, while only two small, barely visible, reflection occur at lower angles. Without their accurate location, peak indexing by TREOR[43] failed, the program being unable to address the correct metrics in the absence of suitably high d values. To overcome these difficulties a variety of strategies can be adopted: i) the parallel use of different indexing approaches which, nowadays, is a (much) easier task;[44] ii) the necessity of trusting low-angle small reflections (often attributed to impurities), particularly after reiterated syntheses and measurements; iii) the accurate detection of low intensity peaks, favored by highly collimated optics and zero-background sample holders.

B_2. Uno, Nessuno, Centomila. During the investigation of the elusive copper(I) imidazolate, we learned of the existence, in the old literature, of a few scattered and incomplete reports on the $Cu(im)_2$ species; this compound immediately appeared to us a very interesting material, from

the structural, spectroscopic, magnetic and bioinorganic points of view. The synthesis itself proved to be a challenging task, since the only structurally characterized species, of blue color (J),[45] could not be resynthesized. Instead, a very controlled approach and a fine tuning of the reaction conditions, eventually afforded several other polymorphs, as *monophasic* samples, easily distinguishable by their colors: Blue (B), Green (G), Olive (O) and Pink (P) (see Figure 8).[46] An amorphous green species was also prepared. Thus, all together, five polymorphs of $Cu(im)_2$ have been detected but only four have been fully characterized by diffraction methods (three from XRPD data), the pink phase still awaiting a structural model.

The structures of these polymorphic species are schematically drawn in Figure 9, where the presence of cavities, tunnels or layers can be easily appreciated. For the sake of completeness, a synoptic table showing the many $Cu(im)_n$ phases detected so far [also thanks to the recently published hydrothermal preparations of some Cu(I) containing phases] is reported. Table 1 nicely illustrates the complex crystal chemistry of the copper-imidazole binary system, which has been recently invoked[47]

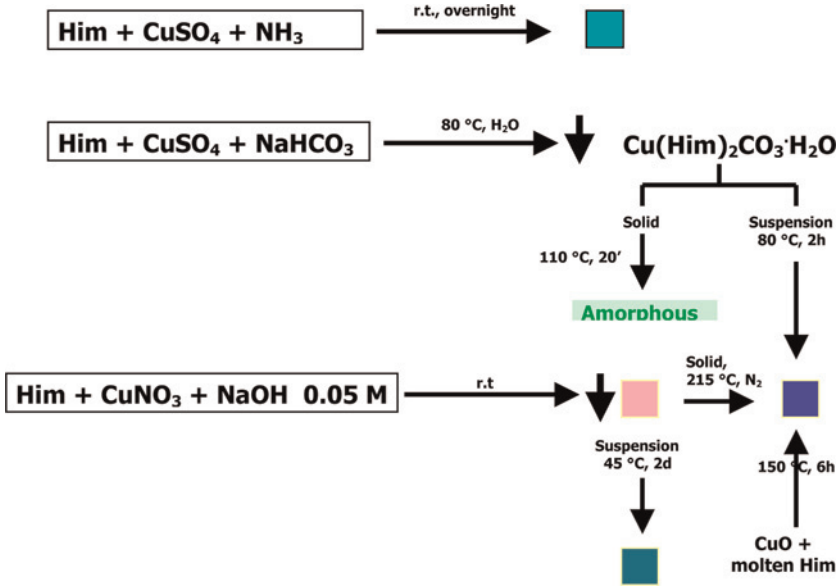

Figure 8. Reaction conditions employed for the preparation of monophasic samples of the different $Cu(im)_2$ polymorphs, each one indicated by a squared color label.

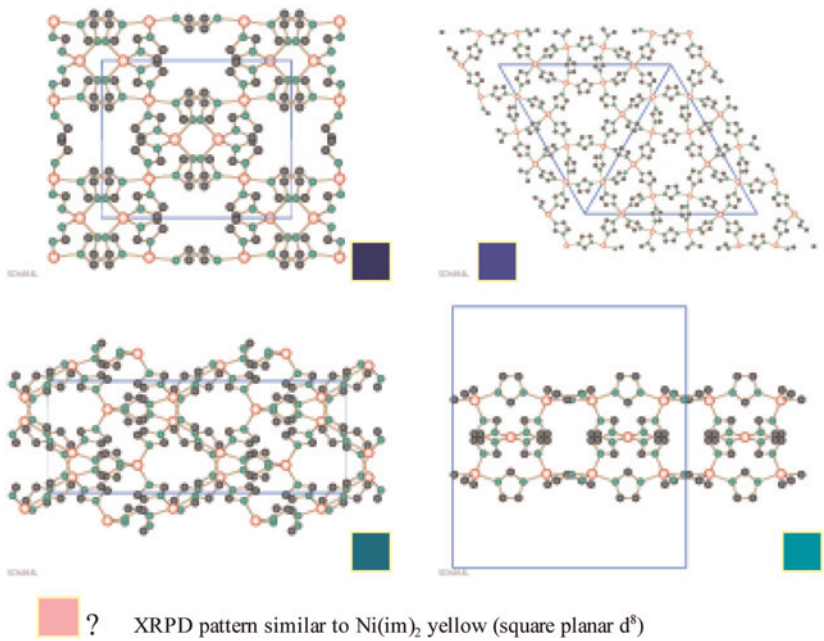

Figure 9. Schematic drawing of the crystal packing of $Cu(im)_2$: left to right, top to bottom: J, B, O and G polymorphs. The structure of the pink (P) phase is still unknown. (The color image is available online at www.taylorandfrancis.com).

Table 1. Synoptic collection of the main structural features of the various $Cu(im)_n$ species

Species	$Cu(im)_2$	$Cu(im)_2$	$Cu(im)_2$	$Cu(im)_2$	$Cu(im)_2$	Cu(im)	Cu(im)	$Cu_2(im)_3$	$Cu_3(im)_4$
Color	Blue	Blue	Green	Olive	Pink	White	Golden	Green	Mauve
SG	I2/c	R-3	Ccca	C2/c	-	-	C2/c	$P2_1/n$	P-1
V/Z, Å^3	180	197	187	201	-	-	180	284	360
ρ, g cm^{-3}	1.824	1.667	1.753	1.632	-	-	2.012	1.914	2.118
Topology	3D	3D	2D	3D	-	-	1D	3D	3D
Topology	PtS	sodalite	slabs	moganite	-	-	Zig-zag	new	NbO
Cavities	NO	Tunnels	NO	Closed	-	-	NO	NO	NO
		7.5%	NO	11%					
Cu atoms	–1	2	222	2			–1	1	–1
site	2		1	1				1	–1
symmetry								1	–1
								1	
Reference	45	46	46	46	46	51	52	53	53

to form very effective anticorrosion layers protecting aerial oxidation of the metal.

As shown above, XRPD is the fundamental tool to be used when polymorphic systems are detected: a) for their quick (qualitative) assessment; b) for their accurate quantitative analysis; and, c) structurally speaking, for retrieving the crystallographic models of samples which, typically, are metastable and, upon manipulation, tend to form (single) crystals of the most stable phase. Consistently, a number of polymorphic systems have been recently studied by us using uniquely XRPD data: $Pd_2(dmpz)_4$ $(Hdmpz)_4$ (Hdmpz = 3,5-dimethylpyrazole),[48] $Cu(bipy)Cl_2$, (bipy = 4,4'-bipyridine)[49] and Acitretin®.[50]

B_3. Interpenetrating Diamondoid Frameworks. $Zn(im)_2$ and $Co(im)_2$, two tetragonal but crystallographically distinct phases, are known since long, contain tetrahedrally coordinated M(II) ions and are extremely complex;[54] at variance, the supramolecular arrangement of the two isomorphous orthorhombic Cd and Hg analogues, recently studied by us using XRPD,[31] is surprisingly simple, being based on the 3D diamondoid network, very common for tetrahedral centers and bidentate spacers. However, imidazolate lacks of "pseudo cylindrical" symmetry and forces short intermetallic distances: thus, its two-fold interpenetration (see Figure 10) is rather unexpected.[55] *Inter alia*, $Cd(im)_2$ and $Hg(im)_2$ are the smallest coordination polymers possessing this peculiar structural feature [apart from inorganic $Zn(CN)_2$]. Interestingly, this topological occurrence cannot be achieved if metals of small(er) ionic radii are employed (Zn, Co and Cu bis-imidazolates).[46,55] Differently, Cd (but not Hg,[24b] due to its peculiar sterochemical requirements) and first-row transition metals (Fe, Co, Cu and Zn)[23,24] tetrahedral bis-pyrazolates, for which interpenetration is not possible, are found to be isomorphous, although not completely miscible.

These two structures were nicely solved by the simulated annealing technique implemented in TOPAS,[56] which, thanks to its powerful graphic routines, allows the real-time estimation of the chemical soundness of the proposed solutions. Worthy of note, the sampling of the whole parameter space is not guaranteed (and never complete) by the random seed generation of the trial structures. Thus rejection or acceptance of a suitable structural model requires coupling of graphical, numerical and visual criteria. The structural features of these two samples, together with their easy chemical preparation, make them ideal candidates for

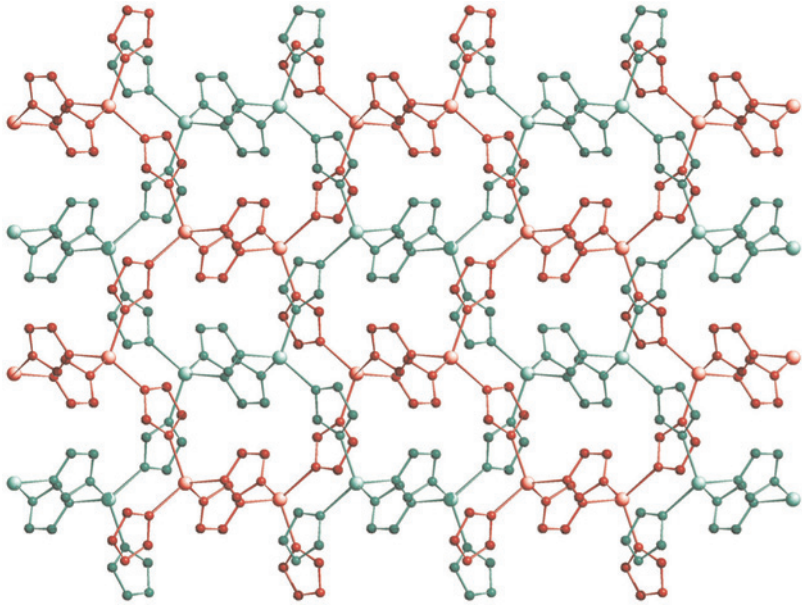

Figure 10. Schematic drawing of the $M(im)_2$ (M = Cd, Hg) species. The two interpenetrating diamondoid frameworks are shown in red and green. (The color image is available online at www.taylorandfrancis.com).

classroom demonstrations, where also the indexing, space group determination and Le Bail intensity extraction steps, as well as Patterson and difference Fourier methods, can be easily tackled.

C. Metal Pyrimidinolates

Hybrid inorganic-organic microporous materials are of particular interest if their properties can be suitably tuned by introducing specific modifications affecting *e.g.* polarity, chirality, etc.; thus, we decided to study the class of trifunctional diazaaromatic species, of which the commercially available 2- and 4-hydroxy-pyrimidines (2- and 4-pymoH) are the simplest precursors. These ligands also offer a wider set of coordination modes, since, in their deprotonated forms, possess three coordination sites (of nearly equal nucleophilicity, thanks to the semiquinoid nature of one of the mesomeric forms). Moreover, their highly polar nature can be further used to influence the stability, and the optical properties (*vide infra*) of the derived frameworks, through interaction with guest molecules (if any).

To our knowledge, the oldest report of a polymeric metal pymo derivative contains the *hydrated* monodimensional polymer, Ag(2-pymo)·$2H_2O$, studied by Quirós back in 1994.[57] Nowadays, several species containing these ligands have been employed in constructing polynuclear *soluble* systems, capable of solution host-guest chemistry and differential recognition of biologically active species.[58] In the following, only *insoluble*, polymeric compounds will be presented, with particular emphasis on the differences between the species derived from the two structural isomers.

C_1. Lord of the Rings. After having studied the syntheses and crystal structures of several group 11 metal azolates (*vide supra*), we learned[57] of the existence of a hydrated polymer, $Ag(2-pymo)\cdot 2H_2O$, whose structure is partially reminiscent of that of the M(pz) (M = Cu, Ag) phases. Accordingly, we decided to attempt the synthesis of the hypothetical Ag(2-pymo) phase by either thermally induced dehydration (monitored by DSC, TGA, IR and XRPD) or directly from anhydrous components.

Upon heating, $Ag(2-pymo)\cdot 2H_2O$ readily loses water in the 80–110°C range ($\Delta H = 101\,kJ\,mol^{-1}$); at higher temperatures, a weak exothermic event, not accompanied by weight losses, is observed at about 150°C ($\Delta H = -4.9\,kJ\,mol^{-1}$), well before the complete thermal decomposition (to metallic silver) occurring at about 300°C. XRPD showed that progressive heating generates an amorphous phase which transforms, above 150°C, into a white (poly)crystalline one (see Figure 11). IR monitoring (nujol mulls) confirmed the loss of water and the formation of a slightly different absorption pattern, which we originally attributed to the anhydrous Ag(2-pymo) polymer. However, rather surprisingly, our XRPD analysis led to the discovery of a novel cyclic, hexameric, chair-like compound $[Ag(2-pymo)]_6$, of crystallographic C_{2h} symmetry.[59]

The silver ions, approximately lying at the vertices of a non-bonded [Ag···Ag 6.117(6) and 5.909(5) Å] hexagon (see Figure 12), are linearly coordinated by nitrogen atoms of the N,N' -bidentate ligands[60] and possess short contacts (of the aurophilic type) with neighbouring molecules [Ag···Ag 2.962(2) and 3.061(5) Å].

On attempting the parallel synthesis of the copper analogue, a highly reproducible, but complex, XRPD pattern of a yellow polycrystalline species [analyzing as Cu(2-pymo)] was repeatedly obtained. Its (lengthy)

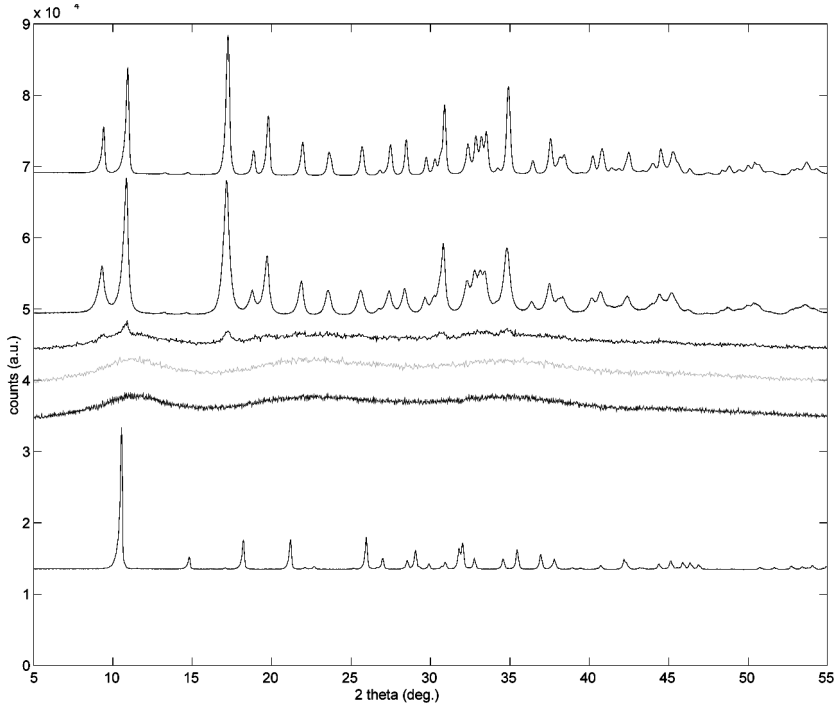

Figure 11. Raw XRPD data showing the Ag(2-pymo)·$2H_2O$ dehydration (and amorphization) process and subsequent devitrification to crystalline $[Ag(2\text{-pymo})]_6$. Bottom to top: as synthesized; 15′, 90°C; 15′, 120°C; 15′, 140°C; 1 h, 190°C; 2 h, 260°C. Note that the top first and second curves possess FWHM's of 0.20° and 0.40° (2θ), respectively.

crystal structure determination eventually led to a structural model containing separate hexamers (Figure 13a) and helical polymers (Figure 13b) in a 1:2 ratio, with digonal copper atoms bound to N,N' -bidentate 2-pymo ligands. Therefore, Cu(2-pymo) should be better described as a $1/6[Cu(2-pymo)]_6 \cdot 1/n[Cu_2(2-pymo)_2]_n$ adduct (stoichiometrically consistent with the original Cu(2-pymo) formulation!). The helices contain six Cu(2-pymo) monomers per turn (with a pitch of 9.79 Å), *i.e.* possess a rare (non-crystallographic) 6_1 (or 6_5) character,[61] and are heavily compenetrated, each being trigonally surrounded by three helices of opposite chirality (see Figure 14). Noteworthy, adjacent helices are displaced by *ca. one third* (and not half) of their pitch; within the space left by the packing of six adjacent helices, a *closed* cavity is formed

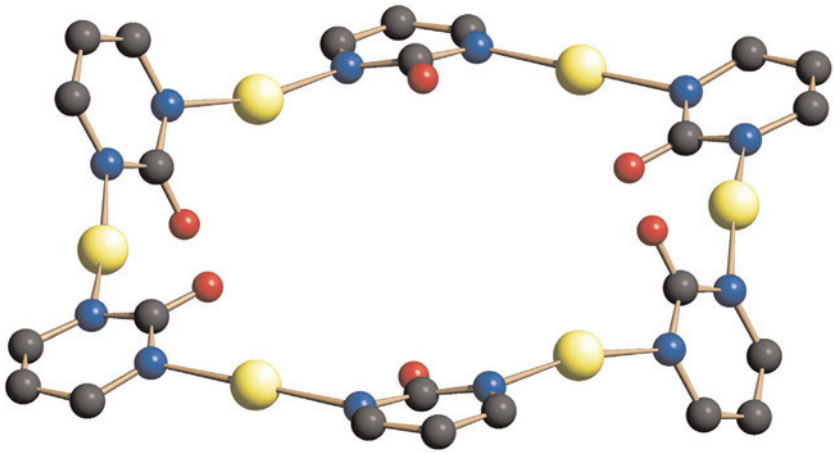

Figure 12. Schematic drawing of the $[Ag(2\text{-pymo})]_6$ molecule, possessing crystallographic C_{2h} symmetry. Note the folded character of the whole ring.

(see Figure 13), which *perfectly* matches the size and shape of $[Cu(2\text{-pymo})]_6$; thus, once filled by the hexamers, the packing of helices in "Cu (2-pymo)" shows no other (solvent accessible) holes.

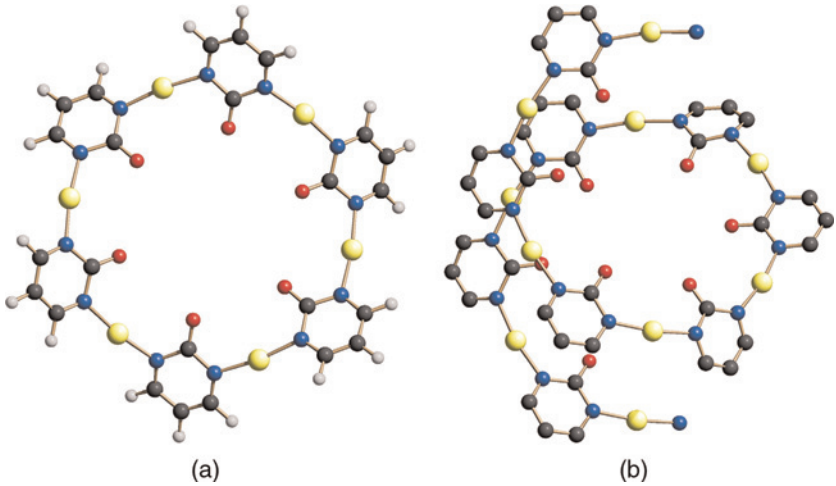

Figure 13. Molecular drawing of (a) the $[Cu(2\text{-pymo})]_6$ hexamer (similar to that found in the silver analogue) and (b) a portion of the infinite helix of $[Cu_2(2\text{-pymo})_2]_n$. (The color image is available online at www.taylorandfrancis.com).

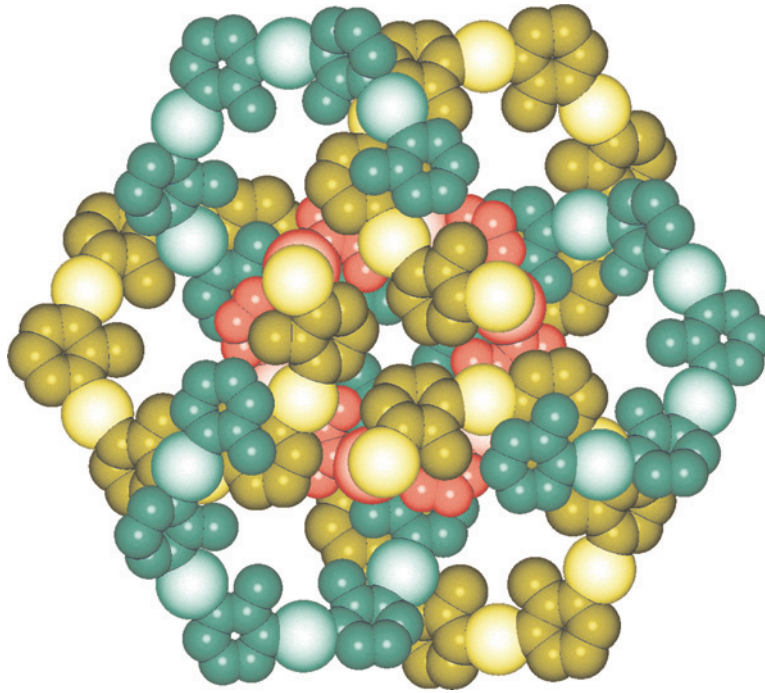

Figure 14. A packing diagram of the $1/6[Cu(2\text{-pymo})]_6 \cdot 1/n[Cu_2(2\text{-pymo})_2]_n$ species, viewed down [001]; helices of different polarity are depicted by different colors (yellow and green); within this trigonal packing of helices, *closed* cavities about the origin host the $[Cu(2\text{-pymo})]_6$ hexamer (red).

These two structure determinations clearly show that, despite the simple M(2-pymo) formulation, the correct stoichiometry, molecular structure and overall supramolecular arrangements, all unforeseen beforehand, were satisfactorily determined by XRPD, even in the presence of broad diffraction peaks [widened by the thermal treatment of the hydrated Ag(2-pymo) polymer] or of a complex pattern (for Cu(2-pymo), where the Laue class, the correct space group and ligand location were partially obscured by, among other effects, the pseudosymmetric arrangement of the heaviest scatterers).

C_2. Some Like it Hot. Thermal stability and chemical inertness are often related, being due to the presence of rather strong intra- and

inter-molecular interactions, to the absence of significantly more stable (oxidation or decomposition) products and/or to the lack of accessible reaction paths. In the case of metal diazolates, thermal decomposition generally leads to metal oxides and nitrides (depending on the conditions employed) or, in some cases, to other inorganic species.[62] Often, some amorphous carbonaceous black material accompanies such decomposition, and the formation of gaseous species (water, CO, CO_2 and HCN) is also observed.

Organic molecular species typically melt, or decompose, at temperatures below 300°C, while a few technologically important polymers were found to be stable up to, typically, 400°C.[63] At first glance surprising, a few metal pyrazolates and imidazolates, particularly those *not* containing metal ions prone to reduction, disproportionation or even ring metalation, were found rather stable, with decomposition temperatures in the 350–450°C range. Accordingly, the very interesting dielectric properties recently discovered for $Zn(im)_2$, were discussed in the frame of potentially useful materials, thanks to the easy method of preparation *and* its high thermal stability and chemical inertness.[47]

Obviously, the presence of stiff heteroaromatic rings, with highly delocalized π systems, and of dipolar interactions in the crystal can be invoked to explain the extreme stability of the $M(2\text{-pymo})_2$ species (M = Co, Ni, Zn), which crystallize as diamondoid frameworks and can be heated *without decomposition* (under N_2) up to *ca*. 550°C.[64] A schematic drawing of the 3D framework of $Co(2\text{-pymo})_2$ is shown in Fig. 15.

Compared to the other known metal(II) diazolates, these metal bis-pyrimidin-2-olates show the highest stabilities: indeed, only $Zn(pz)_2$ was found to sustain such high temperatures. That 2-pymo ligands tend to form rather stable metal adducts was already observed for metal complexes in lower oxidation states, such as Cu(I) and Ag(I): indeed, the complex "Cu(2-pymo)" species discussed above decomposed 70°C higher than α-Cu(pz) (dec. 270°C[10]) and the *hexameric* $[Ag(2\text{-pymo})]_6$ is stable up to 300°C, about 40°C higher than the Ag(pz)[10] and Ag(im)[36] polymers.

The acentric nature of the three $M(2\text{-pymo})_2$ species was confirmed by the measurement of SHG activities of a few percent of standard urea powder. Thus, thermal stability, in these species, is nicely accompanied by potentially useful optical properties, opening the way to a class of new polyfunctional materials.

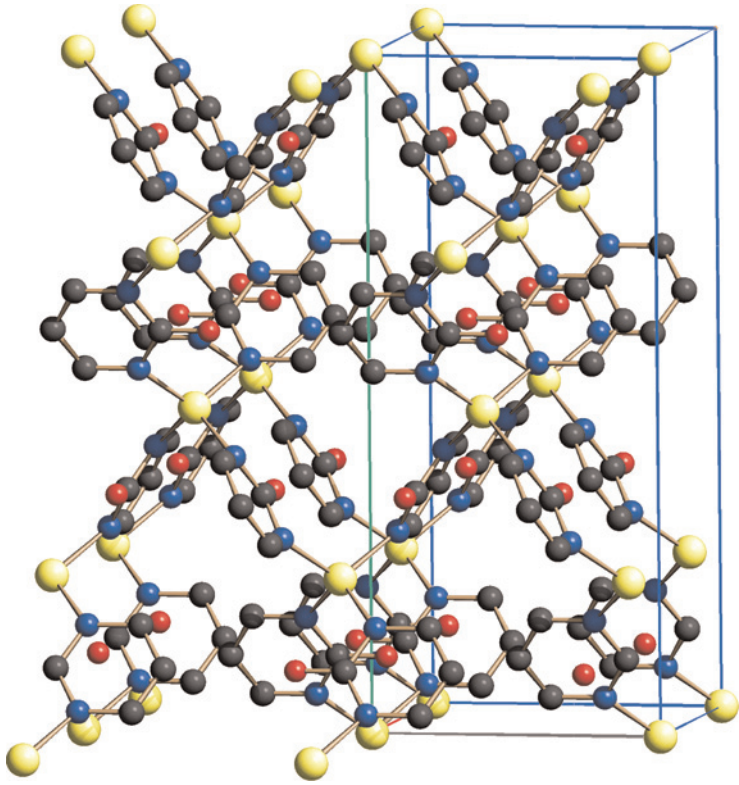

Figure 15. Partial drawing of the 3D diamondoid network in $Co(2\text{-pymo})_2$. (The color image is available online at www.taylorandfrancis.com).

In conventional single crystal diffractometry, acentric crystals normally require a larger number of "independent" diffraction data, including Friedel pairs, and the estimate of the correct enantiomorph by anomalous scattering (if applicable); the determination of the correct set of phases in the starting model also requires longer computational times, and fake solutions are slightly more often encountered. Thus, acentricity is normally thought as an annoying, although not removable, effect. While these observations (more or less) apply also to powder diffractometry, there is at least one step, i.e. indexing, which is (enormously) favored by acentricity: indeed, for a crystal phase containing N crystallographically independent atoms (say, a full molecule), the cell volume is smaller for the acentric, vs. centric, unit cell. Inherently, the indexing procedure is much simpler, and can also benefit

from the lower number of systematic absences conditions, normally increasing the low-angle observable lines (and the resulting figures of merit).

C_3. Magnetically Active Two-dimensional and Three-dimensional Systems. Unsubstituted pyrimidine bridging ligands have been shown to efficiently transmit ferromagnetic interactions in a cobalt(II) layered compound.[65] Thus, in order to prepare magnetically active Co(II) 2D and 3D polymers, we employed the 2-pymo and 4-pymo ligands, which, at variance from pyrazolates, cannot give chain polymers,[23] in the syntheses of extended systems of $Co(2\text{-pymo})_2$[64] and $Co(4\text{-pymo})_2$[66] formulation. The formation of these binary species follows different routes, a stable hydrated intermediate, $Co(4\text{-pymo})_2(H_2O)_4$, being invariably recovered in the latter case. As described above, $Co(2\text{-pymo})_2$ contains N,N′-*exo*bidentate heterocyclic ligands (and crystallizes as a 3D diamondoid framework); at variance, $Co(4\text{-pymo})_2$, obtained by heating above 320°C the aqua species (in the 150–320°C temperature range an anhydrous amorphous phase is formed), surprisingly showed a crystal structure based upon stacking of two-dimensional layers of square meshes defined by 4-pymo ligands in their N,O-*exo*bidentate (not chelating!) mode (see Figure 16). Actually, the metal coordination is completed by ancillary, weak(er) Co···N contacts. Incidentally, the chemistry of the nickel analogues is essentially the same, since, under similar conditions, the $Ni(2\text{-pymo})_2$, $Ni(4\text{-pymo})_2(H_2O)_4$ and $Ni(4\text{-pymo})_2$,[67] isostructural with the cobalt species, were isolated.[68]

Of these species, the most attractive was found to be $Co(2\text{-pymo})_2$, which can be considered a molecular magnet. Indeed, below a critical temperature ($T_c = 23$ K), a ferromagnetic ordering takes place (coercitive field $H_{coer} = 3900$ G, remnant magnetization $M_{rem} = 279\ cm^3\ G\ mol^{-1}$, as determined from the magnetic hysteresis loop, measured at 4.8 K, shown in Fig. 17).

The remaining cobalt species, including the amorphous material of $Co(4\text{-pymo})_2$ formulation, show only much weaker magnetic interactions; the bridging 4-pymo ligands cause, in $Co(4\text{-pymo})_2$, an antiferromagnetic exchange between the *pseudo*tetrahedral cobalt(II) ions with $|J| = 1.73(1)\ cm^{-1}$, which is increased to about $4.1\ cm^{-1}$ in the nickel analogue; in the aqua-(4-pymo) species, magnetically isolated (Co^{2+}) or weakly interacting ions [$J = -0.313(5)\ cm^{-1}$, for Ni^{2+}] are present. Worthy of note, these species are among the few magnetically active

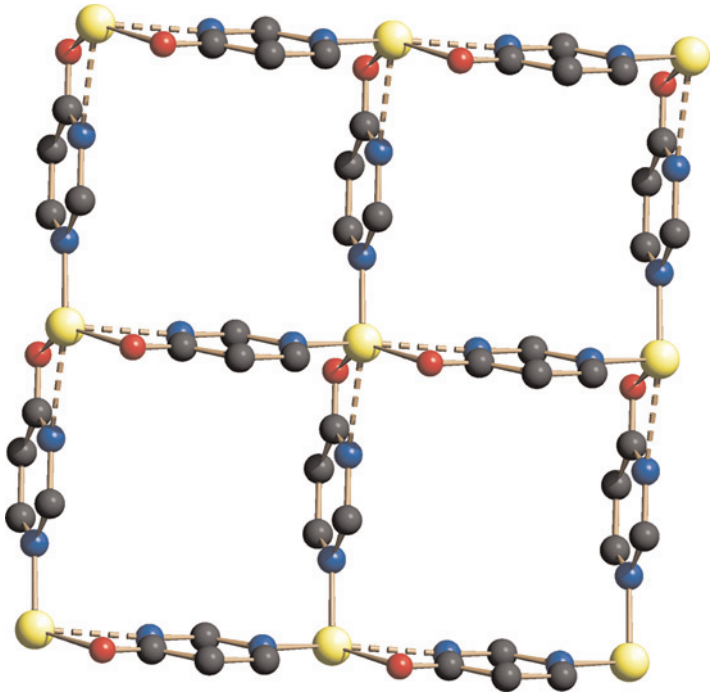

Figure 16. Partial drawing of the 2D network in $Co(4\text{-pymo})_2$. Fragmented lines address the loose (ca. 2.30 Å) Co···N contacts. (The color image is available online at www.taylorandfrancis.com).

compounds which have been characterized by XRPD methods. A detailed list can be found in Ref. 69.

C_4. Mineralomimetic Coordination Frameworks. The wide range of applications of zeolites and phyllosilicates is closely related to their well defined porous nature with concomitant selective ion exchange, sorptive and catalytic processes.[70] Since the mid-1990s a great interest is being paid to the design of extended open-metal-organic-frameworks (MOFs), which mimic the properties of conventional porous solids and, at the same time, overcome their limitations.[71] Thus, in contrast to aluminosilicates, MOFs can be designed at will[72] to control their shape,[73] functionalization, flexibility[74] and, additionally, chirality.[75] Accordingly, we have recently reported a group of neutral and flexible 3D sodalite type MOFs of formula CuL_2 (with L = 2-pymo[76a,c] or 4-pymo[76b]), in which

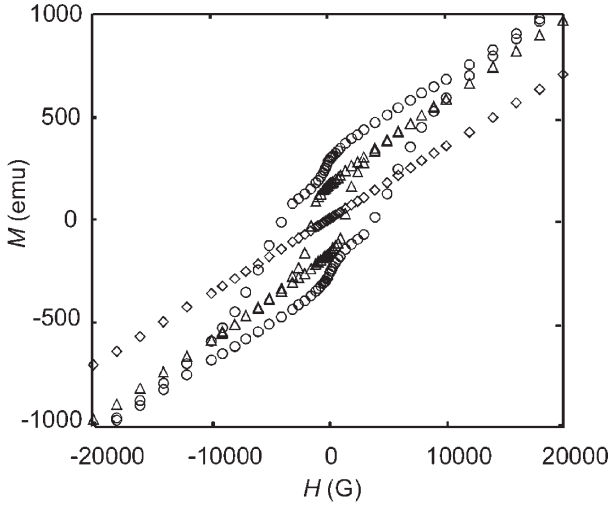

Figure 17. Magnetic hysteresis loops for Co(2-pymo)$_2$ at 5 K (o), 20 K (Δ) and 30 K (◇).

the overall structural features are nearly independent on the position of the exocyclic oxygen atom while shape, size, hydrophilicity and ion pair affinity of the cavities are highly affected.

Cu(2-pymo)$_2$ **(CuP)** showed excellent ion pair recognition properties. Indeed, heterogeneous solid-liquid sorption processes are responsible for an unexpected wide variety of guest-induced crystal-to-crystal phase transitions taking place in the MOF host, which are highly dependent on liquid phase polarity and nature of the guests. Thus, the sorption selectivity of **CuP** for ion pairs containing ammonium or alkali cations and "cubic" anions $(ClO_4^-,\ BF_4^-\ PF_6^-)$ from aqueous solutions[76a] is extended to a wider range of ion pairs containing D_{3h} NO_3^- anions when the solvent polarity is slightly reduced ($MeOH/H_2O$ or $EtOH/H_2O$ mixtures).[76c] Additionally, the novel sorption processes were found to induce profound structural changes in the original **CuP** MOF (Figure 18).[76c]

XRPD showed that the hydrated Cu(2-pymo)$_2$ is *rhombohedral* **(CuP$_R$)** with a distorted 3D sodalite type framework (Figure 18). This 3D framework is not rigid but, upon exposition to a solution of MNO_3 ($M = NH_4$, Li) in aqueous MeOH, a transition to a *cubic* phase, $Cu(2-pymo)_2 \cdot (MNO_3)_{1/3}$ **(MNO_3@CuP$_C$)**, is observed.[77] Single crystal X-ray studies performed on the **MNO_3@CuP$_C$** systems with $M = NH_4$ and Li show that they contain a *regular* sodalite Cu(2-pymo)$_2$

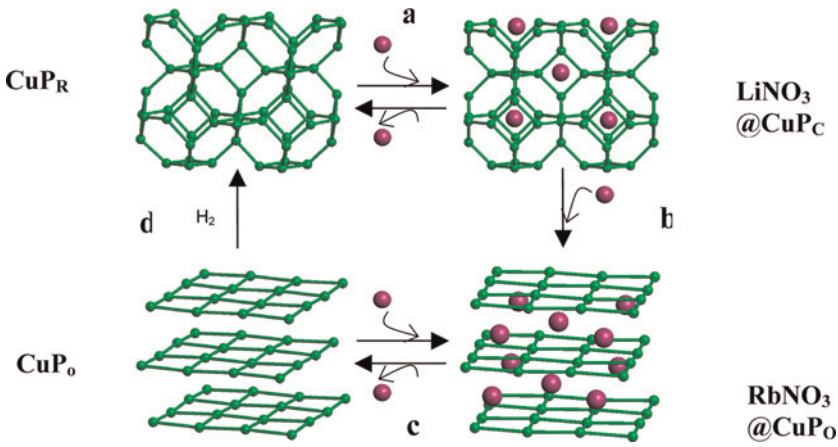

Figure 18. Guest induced transformations in the Cu(2-pymo)$_2$ (**CuP$_R$**) framework. (a) incorporation of n/3 MNO_3. (b) Additional incorporation of 1/6 MNO_3. (c) Removal of 1/2 MNO_3. (d) Water addition. For M's, see text. The balls and sticks denote Cu and pyrimidin-2-olate-*N*,*N*′-bridges, respectively. Coordinates from the crystal structures of **CuP$_R$**, **LiNO$_3$@CuP$_C$** and **RbNO$_3$@CuP$_O$**.

MOF (**CuP$_C$**) with water molecules and $LiNO_3$ or NH_4NO_3 ionic pairs included in the hexagonal channels (Figure 19a). A related structural phase change from the rhombohedral phase (**CuP$_R$**) to the cubic one (**CuP$_C$**) takes also place upon dehydration by heating over 60–70°C (Figure 20). These processes are fully reversible, *i.e.* exposition to water of both **CuP$_C$** and **MNO$_3$@CuP$_C$** restore **CuP$_R$**.

Much more pronounced structural changes take place upon exposition of **CuP$_R$** to methanol solutions of nitrate salts of larger cations (Na^+, K^+, Rb^+, Tl^+); the kinetically controlled crystal-to-crystal inclusion process from **CuP$_R$** to **MNO$_3$@CuP$_C$** is, indeed, followed by further incorporation of 1/6 MNO_3, leading to a novel series of isomorphous *orthorhombic* layered materials, Cu(2-pymo)$_2 \cdot (MNO_3)_{1/2}$ (**MNO$_3$@CuP$_O$**) (Figure 18). **RbNO$_3$@CuP$_O$** consists (single-crystal data) of square grid Cu(2-pymo)$_2$ 2D layers, with the Rb^+ ions coordinated to the pyrimidine exocyclic oxygen atoms of the metallacalix[4]arene (Figure 19b). The MNO_3 guests can be easily removed, giving an *empty layered orthorhombic* Cu(2-pymo)$_2$ species (**CuP$_O$**), which can be further converted into the original **CuP$_R$** phase by exposure to water for a few hours. Thus, the mineralomimetic nature of these systems is related to the topology and functionality of the host MOF's which, like

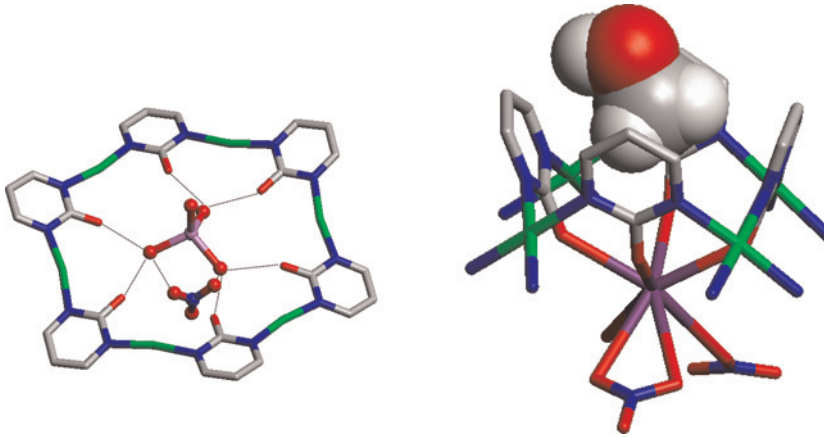

Figure 19. (a) Li^+ coordination in the hexagonal windows of the sodalite β-cages in $\mathbf{LiNO_3@CuP_C}$. (b) The metallacalix[4]arene motif in $\mathbf{RbNO_3@CuP_O}$: the lower-rim recognizes $RbNO_3(H_2O)$, the cone cavity MeOH. Li (purple), Rb (purple), Cu (green), O (red), N (blue), C (grey) and H (white). (The color image is available online at www.taylorandfrancis.com).

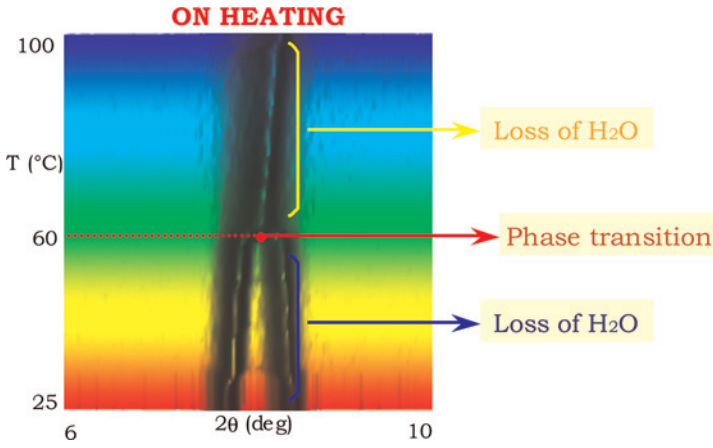

Figure 20. Variable temperature XRPD traces in the 6–10° 2θ range, showing the progressive merging of the 110 and 012 peaks of $\mathbf{CuP_R}$ [a = 23.040(2), c = 25.140(2) Å], into the 110 reflection of the cubic $\mathbf{CuP_C}$ phase (a_0 = 15.07 Å). Vertical scale, T in the 25–100°C range (bottom to top, 10 scans per 10°C interval). Note that, at each T, equilibrium was fully reached. Coalescence occurs at 60°C. (The color image is available online at www.taylorandfrancis.com).

in sodalite (CuP_R and CuP_C) or in talc or muscovite (CuP_O), can intercalate neutral molecules or metal ions, in the cavities or between the layers,[78] respectively.

These latter studies have been performed using a cheap temperature-controlled sample holder,[79] which, thanks to the Peltier battery technology, can cool (down to $-20^{\circ}C$) or heat (up to $160^{\circ}C$) the deposited powders with programmable linear gradients and $\pm 0.1^{\circ}C$ stability. The detection and characterization of sample dehydration processes (which, inter alia, is an extremely important feature during drug development and formulation in pharmaceutical industry) is thus straightforward.

CONCLUSIONS AND OUTLOOK

Polymeric metal diazolates (pyrazolates, imidazolates, pyrimidin-X-olates, X = 2,4) typically appear as insoluble and intractable powders. However, we have shown in this review that the complete retrieval of their structures, using *ab-initio* X-ray powder diffraction methods and well tuned laboratory diffractometers, is nowadays possible. This methodology has been successfully applied to more than 30 species of this class, and not only benchmark (fortunate) case structures. Accordingly, the results schematically presented above on a large class of coordination polymers, structurally characterized by *ab-initio* XRPD, clearly demonstrate that powder diffraction is indeed a very efficient and powerful tool in the structural chemist's hand (once properly employed with tailored software resources) for the complete understanding of the origin of a number of functional properties, such as thermal, optical, magnetic and sorption behavior.

However, it must be continuously stressed that the structural "details" which can be obtained by powder diffraction are rather blurred; nevertheless, XRPD still affords a plenty of useful, otherwise inaccessible, information, such as molecular shape, heavy atoms stereochemistry, rough bonding parameters, crystal packing and nature of paracrystallinity effects. Even if these were the only attainable results, XRPD would be considered an unavoidable source of structural information and a fruitful complement to other structural techniques. Of even higher importance, as recently reviewed,[80] the availability of ancillary methods (of the experimental or even computational type: selected-area electron and/or neutron diffraction, NMR, steric energy estimates, etc.) can further improve the "defocused" structural image retrieved by the

ab-initio XRPD process, and, therefore, should be employed whenever a "higher resolution picture" of the structure, *which XRPD alone cannot afford*, is sought.

According to the results reported above, and to the slow, but steady, increase of crystal structures solved and refined, *uniquely*, from powder diffaction data,[81] more than ever, we feel that the *ab-initio* XRPD method will soon be incorporated in the research activity of a number of laboratories (dealing with, *e.g.*, polymeric functional materials, molecular magnets, catalysts, pharmacologically active species, etc.), as well as in the classrooms of chemistry, physics and material science students.

ACKNOWLEDGEMENTS

We thank all co-workers who have participated in this project for their continuous support and helpful discussions. The Italian MURST, CNR, University of Insubria (Progetto di Eccellenza Sistemi Poliazotati), the Fondazioni Provinciale Comasca and Cariplo are acknowledged for funding.

REFERENCES

1. Generally, 2θ, $\sin\theta$, t, or $1/d$, depending on the nature of the experiment (angle *vs.* energy dispersive diffraction, time-of-flight, etc.).
2. Pecharsky, V. K., P. Y. Zavalij, Fundamentals of Powder Diffraction and Structural Characterization of Materials, Kluwer Acad. Pub., Boston, MA, 2003; Crystal Structure Determination from Powder Diffraction, Clearfield, A. Ed., Amer. Cryst. Assoc., 37, 2002.
3. *Powder Diffraction of Molecular Functional Materials*, Masciocchi, N. Ed., IUCr, CPD Newsletters No. 31, 2004.
4. La Monica, G., G. A. Ardizzoia, 1997. *Prog. Inorg. Chem.*, **46**, 151, and references therein.
5. (a) Perera, J. R., M. J. Neeg, H. B. Schlegel, C. H. Winter, 1999. *J. Amer. Chem. Soc.*, **121**, 4536; (b) Gust, K. R., J. E. Knox, M. J. Heeg, H. B. Schlegel, C. H. Winter, 2002. *Eur. J. Inorg. Chem.*, 2327.
6. See, for example: Deacon, G. B., A. Gitlits, P. W. Roesky, M. R. Bürgstein, K. C. Lim, B. W. Skelton, A. H. White, 2001. *Chem. Eur. J.*, **7**, 127, and references therein.
7. Barron, A. R., G. Wilkinson, M. Motevalli, M. B. Hursthouse, 1985. *Polyhedron*, **4**, 1131.
8. Büchner, E. 1889. *Ber. Dtsch. Chem. Ges.*, **22**, 842.
9. Trofimenko, S. 1972. *Chem. Rev.*, **72**, 497, and references therein.

10. Masciocchi, N., M. Moret, P. Cairati, A. Sironi, G. A. Ardizzoia, G. La Monica, 1994. *J. Amer. Chem. Soc.*, **116**, 7768.
11. The increase of the "tolerated" cell volume is reflected by the simultaneous appearance of extra-peaks in calculated positions, not matched by observable diffracted intensity. However, if the space group symmetry imposes several systematic absence conditions, the required set of observable peaks (at low-2θ) is not significally augmented. This was indeed the case for the *Pbcn* space group of the silver trimer.
12. Cascarano, G., L. Favia, C. Giacovazzo, 1992. *J. Appl. Crystallogr.*, **25**, 310.
13. Dinnebier, R. E., F. Albrich, S. VanSmaalen, P. W. Stephens, 1997. *Acta Crystallogr.*, **B53**, 153.
14. Unless the few, possibly weak, "unindexable" peaks are attributed to a known contaminant phase.
15. (a) Kahn, O., J. Kröber, C. Jay, 1992. *Adv. Mater.*, **4**, 718; (b) Garcia, Y., P. van Koningsbruggen, E. Codjovi, R. Lapouyade, O. Kahn, L. Rabardel, 1997. *J. Mater. Chem.*, **7**, 857.
16. Gütlich, P., Y. Garcia, H. A. Goodwin, 2000. *Chem. Soc. Rev.*, **29**, 419.
17. van Koningsbruggen, P. J., Y. Garcia, E. Codjovi, R. Lapouyade, O. Kahn, L. Fournès, L. Rabardel, 1997. *J. Mater. Chem.*, **7**, 2069.
18. (a) Jung, O.-S., C. G. Pierpont, 1994. *J. Am. Chem. Soc.*, **116**, 2229; (b) Jung, O.-S., Y.-A. Lee, C. G. Pierpont, 1995. *Synth. Met.*, **71**, 2019.
19. Smit, E., B. Manoun, S. M. C. Verryn, D. de Waal, 2001. *Powder Diffr.*, **16**, 37.
20. (a) Vos, J. G., W. L. Groeneveld, 1997. *Inorg. Chim. Acta*, **23**, 123; (b) Vos, G., R. A. le Fêbre, R. A. G. de Graaff, J. G. Haasnot, J. Reedijk, 1983. *J. Am. Chem. Soc.*, **105**, 1682; (c) Garcia, Y., P. J. van Koningsbruggen, G. Bracic, P. Guionneau, D. Chasseau, G. L. Cascarano, J. Moscovici, K. Lambert, A. Michalowicz, O. Kahn, 1997. *Inorg. Chem.*, **136**, 6357; (d) Michalowicz, A., J. Moscovici, J. Charton, F. Sandid, F. Benamrane, Y. Garcia, 2001, *J. Synch. Rad.*, **8**, 701.
21. van Koningsbruggen, P. J., Y. Garcia, O. Kahn, L. Fournès, H. Koijman, A. Spek, J. G. Haasnoot, J. Moscovici, K. Provost, A. Michalowicz, F. Renz, P. Gütlich, 2000. *Inorg. Chem.*, **39**, 1891.
22. With the notable exceptions of the bispyrazolate-iron(II) (Patrick, B. O., W. M. Reiff, V. Sánchez, A. Storr, R. C. Thompson, 2001. *Polyhedron*, **20**, 1577) and bis(1-methyl-2-thioimidazolate)iron(II) (Rettig, S. J., V. Sánchez, nchez, A. Storr, R. C. Thompson, J. Trotter, 1999. *Inorg. Chem.*, **38**, 5920) polymers, containing tetrahedral d^6 ions, the structures of which have been recently correlated to their magnetic properties.
23. Masciocchi, N., G. A. Ardizzoia, S. Brenna, G. LaMonica, A. Maspero, S. Galli, A. Sironi, 2002. *Inorg. Chem.*, **41**, 6080, and references therein.
24. See also: (a) $Cu(pz)_2$: Ehlert, M. K., S. J. Rettig, A. Storr, R. C. Thompson, J. Trotter, 1989. *Can. J. Chem.*, **67**, 1970; (b) $Zn(pz)_2$ and $Cd(pz)_2$: Masciocchi,

N., G. A. Ardizzoia, A. Maspero, G. LaMonica, A. Sironi, 1999. *Inorg. Chem.*, **38**, 3657.
25. This is particularly true when substituted polyazoles and non-coordinating anions are used instead of the simple pyrazolate, the packing density of the polymers being lowered by side chains, anions and, in some cases, solvent molecules.
26. Kröber, J., E. Codjovi, O. Kahn, F. Grolière, C. Jay, 1993. *J. Am. Chem. Soc.*, **115**, 9810.
27. van Koningsbruggen, P. J., Y. Garcia, E. Codjovi, R. Lapouyade, O. Kahn, L. Fournès, L. Rabardel, 1997. *J. Mater. Chem.*, **7**, 2069.
28. Kuroiwa, K., T. Shibata, A. Takada, N. Nemoto, N. Kimizuka, 2004. *J. Amer. Chem. Soc.*, **126**, 2016.
29. Similarly, in computational chemistry, large residues are often substituted by simpler isolobal fragments, aiming to a significant reduction of computing times.
30. Masciocchi, N., F. Ragaini, S. Cenini, A. Sironi, 1998. *Organomet.*, **17**, 1052.
31. Masciocchi, N., G. A. Ardizzoia, S. Brenna, F. Castelli, S. Galli, A. Maspero, A. Sironi, 2003. *Chem. Commun.*, 2018.
32. Ribar, B., M. Matkovic, F. Sljukic, F. Gabela, 1971. *Z. Kristallogr.* **134**, 311.
33. Yélamos, C., K. R. Gust, A. G. Baboul, M. J. Heeg, H. B. Schlegel, C. H. Winter, 2001. *Inorg. Chem.*, **40**, 6451; (b) Mösch-Zanetti, N.C., M. Ferbinteanu, J. Magull, 2002. *Eur. J. Inorg. Chem.*, 950.
34. Zheng, W., M. J., Heeg, C. H. Winter, 2003. *Angew. Chem., Int. Ed.*, **42**, 2761 and references therein.
35. Ohtsu, H., I. Shinobu, S. Nagatomo, T. Kitagawa, S. Ogo, Y. Watanabe, S. Fukuzumi, 2000. *Chem. Commun.*, 1051 and references therein.
36. Masciocchi, N., M. Moret, P. Cairati, A. Sironi, G. A. Ardizzoia, G. La Monica, 1995. *J. Chem. Soc. Dalton Trans.*, 1671.
37. Bauman, J. E., Jr., J. C. Wang, 1964. *Inorg. Chem.*, **3**, 368; (b) Sigwart, C., P. Kroneck, P. Hemmerich, 1970. *Helv. Chim. Acta*, **53**, 177.
38. Buck, M., private communication.
39. http://www.portfolio.mvm.ed.ac.uk/studentwebs/session2/group29/infdru.htm.
40. See for example: Nomiya, K., K. Tsuda, T. Sudoh, M. Oda, 1997. *J. Inorg. Biochem.*, **68**, 39.
41. Ardizzoia, G. A., S. Brenna, F. Castelli, S. Galli, G. LaMonica, N. Masciocchi, A. Maspero, 2004. *Polyhedron*, **23**, 3063.
42. Ardizzoia, G. A., G. LaMonica, A. Maspero, M. Moret, N. Masciocchi, 1997. *Inorg. Chem.*, **36**, 2321.
43. Werner, P. E., L. Eriksson, M. Westdahl, 1985. *J. Appl. Crystallogr.*, **18**, 367.
44. Shirley, R. 2002. *The Crysfire 2002 System for Automatic Powder Indexing: User's Manual*, The Lattice Press, Surreys, England.

45. Jarvis, J. A. J., A. F. Wells, 1960. *Acta Crystallogr.*, **13**, 1027.
46. Masciocchi, N., Bruni, S., E. Cariati, F. Cariati, S. Galli, A. Sironi, 2001. *Inorg. Chem.*, **40**, 5897.
47. Gasparač, R., E. Stupnišek-Lisac, C. R. Martin, "Imidazole and its Derivatives as Inhibitors for Prevention of Corrosion of Copper," in Electrochemical Approach to Selected Corrosion and Corrosion Control Studies, P. L. Bonora and F. Deflorian, Eds., EFC Book Series No. 28, 2000, pp. 20–36.
48. Masciocchi, N., G. A. Ardizzoia, G. LaMonica, M. Moret, A. Sironi, 1997. *Inorg. Chem.*, **36**, 449.
49. Masciocchi, N., P. Cairati, L. Carlucci, G. Mezza, G. Ciani, A. Sironi, 1996. *J. Chem. Soc. Dalton Trans.*, 2739.
50. Malpezzi, L., N. Masciocchi, A. Sironi, 2005. *J. Pharm. Sci.*, in press.
51. Powder Diffraction File, ICDD, Swarthmore, PA, PDF No. 52-2401.
52. Tain, Y. Q., H. J. Xu, L. H. Weng, Z. X. Chen, D. Y. Zhao, X. Z. You, 2004. *Eur J. Inorg. Chem.*, 1813.
53. Huang, X. C., J. P. Zhang, Y. Y. Lin, X. L. Yu, X. M. Chen, 2004. *Chem. Commun.*, 1100.
54. (a) Sturm, M., F. Brandel, D. Engel, W. Hoppe, 1975. *Acta Crystallogr.*, **B31**, 2369; (b) Lehnert, R., F. Seel, 1980. *Z. Anorg. Allg. Chem.*, **464**, 187.
55. Very recently, $Cd(im)_2$ was also prepared by solvothermal methods, and found to be strongly photoluminescent: Tian, Y.Q., L. Xu, C. X. Cai, J. C. Wei, Y. Z. Li, X. Z. You, 2004. *Eur. J. Inorg. Chem.*, 1039.
56. TOPAS-R, v. 3.1, Bruker AXS, Karlsruhe, Germany, 2003.
57. Quirós, M. 1994. *Acta Crystallogr.*, **C50**, 1236.
58. Navarro, J. A. R., E. Fresinger, B. Lippert, 2000. *Inorg. Chem.*, **39**, 2301; Barea, E., J. A. R. Navarro, J. M. Salas, M. Quirós, M. Willermann, B. Lippert, 2003. *Chem. Eur. J.*, **9**, 4414.
59. Masciocchi, N., E. Corradi, M. Moret, G. A. Ardizzoia, A. Maspero, G. La Monica, A. Sironi, 1997. *Inorg. Chem.*, **36**, 5648.
60. The possibility of an N,O-coordination, similar to that found in the $[Cu(mpyo)]_4$ (Hmpyo = 2-hydroxy-6-methylpyridine) tetramer [Berry, M., Clegg, W., Garner, C. D., Hillier, I. H. 1982. *Inorg. Chem.*, 21, 1342], was also originally considered, but IR evidences, hard/soft acid/base considerations and successful refinement led to a more plausible N,N'-link.
61. See, for example: Batten, S. R., B. F. Hoskins, R. Robson, 1997. *Angew. Chem., Int. Ed. Engl.*, 636; Withersby, M. A., A. J. Blake, N. R. Champness, P. Hubberstey, W. S. Li, M. Schroeder, 1997. *Angew. Chem., Int. Ed. Engl.*, **36**, 2327.
62. For instance, $Zn(CN)_2$ is quantitatively recovered in pure crystalline form from thermal decomposition of zinc bispyrazolate, with concomitant acetonitrile extrusion.

63. See, for example, the poly(*p*-hydroxybenzoic) acid (PHBA): Yoon, D.Y., N. Masciocchi, L. E. Depero, C. Viney, W. Parrish, 1990. *Macromol.*, **23**, 1793.
64. Masciocchi, N., G. A. Ardizzoia, G. LaMonica, A. Maspero, A. Sironi, 2000. *Eur. J. Inorg. Chem.*, 2507.
65. Lloret, F., G. De Munno, M. Julve, J. Cano, R. Ruiz, A. Caneschi, 1998. *Angew. Chem., Int. Ed. Engl.*, **318**, 2781.
66. Masciocchi, N., S. Galli, A. Sironi, E. Barea, J. A. R. Navarro, J. M. Salas, L. C. Tabares, 2003. *Chem. Mater.*, **15**, 2153.
67. Actually, another hydrated phase, $Ni(2\text{-pymo})_2(H_2O)_{2.5}$, absent in the cobalt(II) system, was found.
68. Barea, E., J. A. R. Navarro, J. M. Salas, N. Masciocchi, S. Galli, A. Sironi, 2004. *Inorg. Chem.*, **43**, 473.
69. Galli, S., N. Masciocchi, A. Sironi, 2004. *J. Phys. Chem. Solids*, **65**, 693.
70. Corma, A., 1997. *Chem. Rev.*, **97**, 2373.
71. See e.g. (a) Yaghi, O. M., M. O'Keeffe, N. W. Ockwig, H. K. Chae, M. Eddaoudi, J. Kim, 2003. *Nature*, **423**, 705; (b) Janiak, C. 2003. *J. Chem. Soc. Dalton Trans.*, 2781.
72. Eddaoudi, M., J. Kim, N. Rosi, D. Vodak, J. Wachter, M. O'Keefe, O. M. Yaghi, 2002. *Science*, **295**, 469.
73. Keller, S. W., S., Lopez, 1999. *J. Amer. Chem. Soc.*, **121**, 6306.
74. Kitaura, R., K. Seki, G. Akiyama, S. Kitagawa, 2003. *Angew. Chem. Int. Ed.*, **42**, 428.
75. Seo, J. S., D. Whang, H. Lee, S. I. Jun, J. Oh, Y. J. Jeon, K. Kim, 2000. *Nature*, **404**, 982; (b) Lee, S. J., W. Lin, 2002. *J. Amer. Chem. Soc.*, **124**, 4554.
76. Tabares, L. C., J. A. R. Navarro, J. M. Salas, 2001. *J. Amer. Chem. Soc.*, **123**, 383. (b) Barea, E., J. A. R. Navarro, J. M. Salas, N. Masciocchi, S. Galli, A. Sironi, 2003. *Polyhedron*, **22**, 3051; (c) Barea, E., J. A. R. Navarro, J. M. Salas, N. Masciocchi, S. Galli, A. Sironi, 2004. *J. Amer. Chem. Soc.*, **126**, 3014.
77. Apart from the evacuated $\mathbf{CuP_C}$ and $\mathbf{CuP_O}$ species, all species host, in their MOF channels, a number of water molecules.
78. Putnis, A. *Introduction to Mineral Sciences*. Cambridge University Press, Cambridge, 1992.
79. Equipped with zero background plates and supplied by Officina Elettrotecnica di Tenno, Italy.
80. Masciocchi, N., Sironi, A. 2005. *Comptes Rendus Chimie*, in press.
81. See, for example, Armel Le Bail's website: http://www.cristal.org/iniref.html.